

Study of Dynamical Properties in Shock & Solitary Structures and its Evolutionary Stages in a Degenerate Plasma

Mainak Chatterjee¹, Meghna Dasgupta², Sayoni Das², Moitreyee Halder² and Swarniv Chandra^{3*}

1 Department of Physics, Barasat Government College, Barasat, West Bengal-700124, India

2 Department of Physics, Acharya Prafulla Chandra College, New Barrackpore, West Bengal-700131, India

3 Department of Physics, Government General Degree College, Kushmandi, Dakshin-Dinajpur-700121, India

**Institute of Natural Sciences and Applied Technology, Kolkata, India, 700032.*

E-mail:mainak216@gmail.com (corresponding author)

The basic aim of this study is to use one dimensional Quantum hydrodynamics model to analyse the solitary profiles and shock fronts of Electrostatic and Ion acoustic waves in semi classical plasma, by using the governing equations to derive the KdV-Burgers equation with the help of standard perturbation techniques and stretching expressions, and then extending the study of the nonlinearities of the ion acoustic waves to obtain the Non Linear Schrodinger's Equation and studying the formation of rogue waves from it, also analyzing the 2D and 3D plots to conclude certain observable and experimental facts. The paper also includes the study of the dynamics of the system and its behavioral changes when subjected to small perturbations.

1. Introduction

There exists a huge number of low and high frequency modes of propagation of the waves in plasma. Two such types of modes are the Electrostatic and Ion acoustic modes. These are low frequency longitudinal plasma oscillation. The ion acoustic wave [1, 2] equation describes the dynamics of collision less plasma made of cold ion and hot electrons. These waves arise because of the restoring force imparted by the electrons' thermal pressure [3], while the effect of inertia is portrayed due to the mass of the ions [4, 5]. In case of electrostatic waves [6], both the electrons and the ions present in the plasma act as oscillating species, and the wave propagation is possible because of these oscillations [7,8]. Many types of nonlinear electrostatic structures [9] could propagate in electron-positron plasmas such as solitary shock, blow-up and rouge waves. Quantum hydrodynamic model is one of the popular ways to describe the dynamics of the plasma particles at quantum scales [10]. This model consists of a set of equations [11] describing the transport of charge carriers, momentum and energy in a charged particle system interacting through a self-consistent electrostatic potential. Shock wave is a type of propagating disturbance [12] that moves faster than the speed of sound. It is generated, when there is an abrupt change in the temperature, pressure or density of a medium. It is a discontinuous surface that connects supersonic and subsonic flow. Entropy increases when a shock wave flows so the flow is an

irreversible process, and the system loses its equilibrium due to this. Shock waves also appear in plasma but differ from normal gas due to the electromagnetic nature of plasma. The shock waves in plasma are generally generated due to the interaction between the moving charged particles and electric or magnetic fields, resulting in the formation of huge electromagnetic forces, which accelerate the ions to Supersonic speeds, thus carrying the shock waves forward. When the flow of plasma is parallel to the magnetic field, shock wave appears in governing equation for velocity potential is in hyperbolic relation with match number [13]. A soliton (solitary / standing wave) in plasma tends to become shock fronts with increasing viscosity of the system. Such shock waves can frequently be seen in the sun's corona in the form of solar flares which shoots the ions with such Supersonic speeds that they reach the earth's outer atmosphere and interact with the planets magnetic fields to generate beautifully colored patterns called the Aurora Borealis. Rouge waves are unusually large, unexpected and suddenly appearing surface waves that can be extremely dangerous [14, 15]. In Oceanography, rouge waves are more precisely defined as waves whose height is more than twice the significant wave height. Rouge waves can occur in media other than water. The rouge waves are observed experimentally in plasma physics, in ocean, in Bose-Einstein condensates, in super-fluid helium etc. In plasma physics, we study rouge waves by solving nonlinear Schrodinger (NLS) equation [16]. Rouge wave suddenly tend to appear and then disappear, without any trace. It can be

created due to nonlinear effect in plasma waves. The study of nonlinear phenomena [17] in plasmas is one of the most important research topics in plasma physics. Formation and propagation of solitary waves, periodic waves are very challenging problems in plasma physics. We can study chaotic motion [18] of nonlinear waves by considering an external perturbation.

The basic motive of our paper is to study one dimensional quantum hydrodynamic model to analyze shock fronts and solitary profile of ion acoustic waves in semi classical plasma, by analyzing the plots of the Dispersion relation and the solutions of the KdV-B equation, and then will carry the work forward to analyze the Rogue wave formation, by deriving the Non Linear Schrodinger's Equation (NLSE) from the solitary part of the KdV-B equation and also study the chaotic motion of nonlinear waves and plotting its solution for further analysis.

2. Basic formulation

A. Governing Equations

Following are the governing equations we are going to use for our study.

$$\frac{\partial(n_e)}{\partial t} + \frac{\partial(n_e u_e)}{\partial x} = 0 \quad (1)$$

$$\frac{\partial(n_i)}{\partial t} + \frac{\partial(n_i u_i)}{\partial x} = 0 \quad (2)$$

$$\left(\frac{\partial}{\partial t} + u_i \frac{\partial}{\partial x}\right)(u_i \gamma_i) = \frac{1}{m_e} \left(Q_i \frac{\partial \phi}{\partial x} + \eta_i \frac{\partial^2 u}{\partial x^2}\right) \quad (3)$$

$$0 = \frac{1}{m_e} \left[Q_e \frac{\partial \phi}{\partial x} - \frac{1}{n_e} \frac{\partial P_e}{\partial x} + \frac{\hbar^2}{2m_e} \frac{\partial}{\partial x} \left(\frac{1}{\sqrt{n_c}} \frac{\partial^2 \sqrt{n_c}}{\partial x^2} \right) + Q_e \frac{\partial(U_{xc,c})}{\partial x} \right] \quad (4)$$

$$\frac{\partial^2 \phi}{\partial x^2} = 4\pi(Q_e n_e + Q_i n_i) \quad (5)$$

Here, $U_{xc,e}$: Exchange Correlation term of Electrons; Q_e : e (Charge of electron= 1.6×10^{-19}); Q_i : $-z_i e$

B. Normalization scheme

$$x \rightarrow x\omega_c/V_{Fh}; t \rightarrow t\omega_c; \phi \rightarrow e\phi/k_B T_{Fh}; n_j \rightarrow n_j/n_{j0};$$

$$n_i \rightarrow n_i/n_{i0}; u_j \rightarrow u_j/V_{Fh}$$

$$V_{Fh} = \sqrt{2k_B T_{Feh}/m_e}; \omega_{ec} = \sqrt{4\pi n_{ec0} e^2/m_e}$$

Using these above normalization schemes, equation (1) to (5) can be written as:

2.1 Electrostatic waves

$$\frac{\partial(n_e)}{\partial t} + \frac{\partial(n_e u_e)}{\partial x} = 0 \quad (6)$$

$$\frac{\partial(n_i)}{\partial t} + \frac{\partial(n_i u_i)}{\partial x} = 0 \quad (7)$$

$$\left(\frac{\partial}{\partial t} + u_i \frac{\partial}{\partial x}\right)(u_i \gamma_i) = -\mu \frac{\partial \phi}{\partial x} + \eta_i \frac{\partial^2 u_i}{\partial x^2} \quad (8)$$

$$0 = \frac{\partial \phi}{\partial x} - \frac{1}{n_e} \frac{\partial P_e}{\partial x} + \frac{\hbar^2}{2} \frac{\partial}{\partial x} \left[\frac{1}{\sqrt{n_e}} \frac{\partial^2 \sqrt{n_e}}{\partial x^2} \right] - \lambda_{1e} n_e^{-\frac{2}{3}} \frac{\partial n_e}{\partial x} + \lambda_{2e} n_e^{-\frac{1}{3}} \frac{\partial n_e}{\partial x} \quad (9)$$

$$\frac{\partial^2 \phi}{\partial x^2} = (n_e - n_i) \quad (10)$$

Where, H is Quantum Diffraction Parameter;

$$\text{And, } \lambda_{1e} = \frac{1.66 e^2 n_{e0}^{\frac{1}{3}}}{3\epsilon E_{Fe}}; \lambda_{2e} = \frac{3.77 \hbar^2 n_{e0}^{\frac{2}{3}}}{m_e E_{Fe}}; \mu = \frac{m_e}{m_i}$$

2.2 Ion-acoustic waves

$$\frac{\partial(n_i)}{\partial t} + \frac{\partial(n_i u_i)}{\partial x} = 0 \quad (11)$$

$$\left(\frac{\partial}{\partial t} + u_i \frac{\partial}{\partial x}\right)(u_i \gamma_i) = -\mu \frac{\partial \phi}{\partial x} + \eta_i \frac{\partial^2 u_i}{\partial x^2} \quad (12)$$

$$\frac{\partial^2 \phi}{\partial x^2} = (n_e - n_i) \quad (13)$$

We use the stretching expression:

$$\xi = \epsilon^{1/2} (x - V_0 t); \tau = \epsilon^{3/2} t; \eta = \epsilon^{1/2} \eta_0$$

$$\frac{\partial}{\partial x} \equiv \epsilon^{1/2} \frac{\partial}{\partial \xi}; \quad \frac{\partial^2}{\partial x^2} \equiv \epsilon \frac{\partial^2}{\partial \xi^2};$$

$$\frac{\partial}{\partial t} \equiv -\varepsilon^{1/2} V_0 \frac{\partial}{\partial \xi} + \varepsilon^{3/2} \frac{\partial}{\partial \tau}$$

C. Classical pressure term

$$P_j = n_j k_B T_j$$

D. The perturbation expansions

$$\begin{bmatrix} n_j \\ u_j \\ \phi \end{bmatrix} = \begin{bmatrix} 1 \\ u_0 \\ \phi_0 \end{bmatrix} + \varepsilon \begin{bmatrix} n_j^{(1)} \\ u_j^{(1)} \\ \phi^{(1)} \end{bmatrix} + \varepsilon^2 \begin{bmatrix} n_j^{(2)} \\ u_j^{(2)} \\ \phi^{(2)} \end{bmatrix} + \varepsilon^3 \begin{bmatrix} n_j^{(3)} \\ u_j^{(3)} \\ \phi^{(3)} \end{bmatrix} + \dots$$

$$n_j = 1 + \varepsilon n_j^{(1)} + \varepsilon^2 n_j^{(2)} + \varepsilon^3 n_j^{(3)} + \dots$$

$$u_j = u_0 + \varepsilon u_j^{(1)} + \varepsilon^2 u_j^{(2)} + \varepsilon^3 u_j^{(3)} + \dots$$

$$\phi = \phi_0 + \varepsilon \phi^{(1)} + \varepsilon^2 \phi^{(2)} + \varepsilon^3 \phi^{(3)} + \dots$$

3. The Dispersion relation

For deriving the dispersion relation of both type of waves, we substitute the perturbation expansions into the normalized sets of equations, and then linearizing and assuming that all the quantities vary simple harmonically as $e^{i(kx - \omega t)}$; and separating the real and imaginary parts, for normalized wave frequency ω and k , we get the equation as:

3.1. Electrostatic waves

$$\omega = u_0 k + i \left(\frac{k}{2} \sqrt{k^2 (\eta_i^2 - \mu H^2) - 4\mu (\lambda_{2e} - \lambda_{1e})} - \frac{\eta_i^2 k^2}{2} \right) \quad (14)$$

When $k < \sqrt{4\mu \frac{(\lambda_{2e} - \lambda_{1e})}{(\eta_i^2 - \mu^2 H^2)}}$, the real part i.e. the

Dispersion Relation is:

$$\omega_r = u_0 k - \frac{k}{2} \sqrt{4\mu (\lambda_{2e} - \lambda_{1e}) - k^2 (\eta_i^2 - \mu H^2)} \quad (15)$$

And the imaginary part i.e. the Damping Relation is:

$$\omega_i = -\frac{\eta_i k^2}{2} \quad (16)$$

But as soon as k reaches the value, $\sqrt{4\mu \frac{(\lambda_{2e} - \lambda_{1e})}{(\eta_i^2 - \mu^2 H^2)}}$

The real part changes to:

$$\omega_r = u_0 k \quad (17)$$

And imaginary part becomes:

$$\omega_i = \left(\frac{k}{2} \sqrt{k^2 (\eta_i^2 - \mu H^2) - 4\mu (\lambda_{2e} - \lambda_{1e})} - \frac{\eta_i^2 k^2}{2} \right) \quad (18)$$

3.2. Ion-Acoustic waves

$$\omega = \left(u_0 k + \frac{\sqrt{4\mu - \eta_i^2 k^4}}{2} \right) - i \frac{\eta_i k^2}{2} \quad (19)$$

Where, at the first glance, the real part appears to be,

$$\omega_r = u_0 k + \frac{\sqrt{4\mu - \eta_i^2 k^4}}{2} \quad (20)$$

And the imaginary part appears to be,

$$\omega_i = -\frac{\eta_i k^2}{2} \quad (21)$$

But, on closure inspection, we find that, (20) and

(21) retain their expressions only as long as $k \leq \sqrt[4]{\frac{4\mu}{\eta_i^2}}$

As soon as k becomes greater than $\sqrt[4]{\frac{4\mu}{\eta_i^2}}$, (20) and

(21) changes to: $\omega_r = u_0 k$ (22)

And,

$$\omega_i = \frac{\sqrt{\eta_i^2 k^4 - 4\mu}}{2} - \frac{\eta_i k^2}{2} \quad (23)$$

The real part of (14) and (19) gives us the dispersion relation, and the imaginary part of (14) and (19) gives us the damping relation.

4. The KdV-Burgers equation

By substituting the stretching expressions and the perturbation terms in the normalized equations, and by using mathematical computational methods and collecting the coefficients of similar powers of, we get these equations:

4.1. Electrostatic wave

$$\frac{\partial n_i^{(1)}}{\partial \tau} + n_i^{(1)} \frac{\partial u_i^{(1)}}{\partial \xi} + u_i^{(1)} \frac{\partial n_i^{(1)}}{\partial \xi} = (V_0 - u_0) \frac{\partial n_i^{(2)}}{\partial \xi} - \frac{\partial u_i^{(2)}}{\partial \xi} \quad (24)$$

$$u_i^{(1)} = (V_0 - u_0) n_i^{(1)} \quad (25)$$

$$\phi^{(1)} = (V_0 - u_0) \left(1 + \frac{3u_0^2}{2c^2}\right) u_i^{(1)} \quad (26)$$

$$\phi^{(1)} = [1 - (\lambda_{1e} + \lambda_{2e})] n_e^{(1)} \quad (27)$$

$$\frac{H^2}{4} \frac{\partial^3 n_e^{(1)}}{\partial \xi^3} + (\lambda_{1e} + \lambda_{2e} - 1) \frac{\partial n_e^{(2)}}{\partial \xi} - \left(\frac{2}{3} \lambda_{1e} - \frac{1}{3} \lambda_{2e}\right) n_e^{(1)} \frac{\partial n_e^{(1)}}{\partial \xi} = 0 \quad (28)$$

$$\frac{\partial^2 \phi^{(1)}}{\partial \xi^2} = (n_e^{(2)} - n_i^{(2)}) \quad (29)$$

4.2 Ion- Acoustic Waves

$$u_i^{(1)} = (V_0 - u_0) \quad (30)$$

$$\frac{\partial n_i^{(1)}}{\partial \tau} + n_i^{(1)} \frac{\partial u_i^{(1)}}{\partial \xi} + u_i^{(1)} \frac{\partial n_i^{(1)}}{\partial \xi} = (V_0 - u_0) \left(\frac{\partial n_i^{(2)}}{\partial \xi} - \frac{\partial u_i^{(2)}}{\partial \xi} \right) \quad (31)$$

$$\phi^{(1)} = \frac{(V_0 - u_0)}{\mu} \left(1 + \frac{3u_0^2}{2c^2}\right) u_i^{(1)} \quad (32)$$

$$\frac{\partial^2 \phi^{(1)}}{\partial \xi^2} = -n_i^{(2)} \quad (33)$$

$$\frac{\partial^2 \phi^{(2)}}{\partial \xi^2} = -n_i^{(3)} \quad (34)$$

Solving them by substitution, elimination and reductive perturbation technique, we obtain the following KdVB equation of the form:

$$\frac{\partial \phi}{\partial \tau} + N \phi \frac{\partial \phi}{\partial \xi} + D \frac{\partial^3 \phi}{\partial \xi^3} - R \frac{\partial^2 \phi}{\partial \xi^2} = 0 \quad (35)$$

Where,

N= Nonlinear coefficient

D= Dispersive coefficient

R= Viscous coefficient

As the stream velocity (v_0) is \ll velocity of light (c); thus, neglecting the relativistic terms we get the expressions of coefficients as:

Electrostatic waves

$$N = \frac{\left(\frac{B}{D_3^3} + \frac{2}{D_1 D_3} + \frac{AC}{D_2^3}\right)}{\left(\frac{1}{D_3 A} + \frac{1}{D_1}\right)} \quad (36)$$

$$D = \frac{\left(1 - \frac{H^2}{4D_2^2}\right)}{\left(\frac{1}{D_3 A} + \frac{1}{D_1}\right)} \quad (37)$$

$$R = \frac{\eta_0}{D_3^2 \left(\frac{1}{D_3 A} + \frac{1}{D_1}\right)} \quad (38)$$

Where,

$$D_1 = \frac{(V_0 - u_0)^2}{\mu}$$

$$D_2 = [1 - (\lambda_{1e} + \lambda_{2e})]$$

$$D_3 = (V_0 - u_0)$$

$$A = (V_0 - u_0)$$

$$B = 1$$

$$C = \left(\frac{2}{3} \lambda_{1e} - \frac{1}{3} \lambda_{2e}\right) u_e^{(1)} = (V_0 - u_0) n_e^{(1)}$$

$$\text{Where } \lambda_{1e} = \frac{1.66e^2 n_{e0}^{\frac{1}{3}}}{3\epsilon E_{Fe}}; \lambda_{2e} = \frac{3.77h^2 n_{e0}^{\frac{2}{3}}}{m_e E_{Fe}}; \mu = \frac{m_e}{m_i}$$

For Ion-Acoustic Waves:

$$N = \frac{3\mu}{2(V_0 - u_0)} \quad (39)$$

$$D = \frac{(V_0 - u_0)^3}{2\mu} \quad (40)$$

$$R = \frac{n_0}{2} \quad (41)$$

The solution of the KdVB equations is given by:

$$\phi = \frac{12D}{N} [1 - \tanh^2(\xi)] - \frac{36R}{15N} \tanh(\xi) \quad (42)$$

We see, that the solution contains two parts,

The first part signifies the solitary part of the wave, and the second part refers to the shock profiles. We notice that the coefficient of 2nd part contains R in the numerator, which is directly proportional to η_0 . Thus, we can say, that with increase in viscosity, the shock profiles become more prominent.

From equation (38) and (41), it is evident, that equation (35) reduces to the KdV equation, given by:

$$\frac{\partial \phi}{\partial \tau} + N\phi \frac{\partial \phi}{\partial \xi} + D \frac{\partial^3 \phi}{\partial \xi^3} = 0 \quad (43)$$

When the viscosity term η_0 becomes zero, thus making $R=0$ in equation (35), giving equation (43), which is nothing but the KdV equation, and displays the solitary profiles of the waves.

[During graphical analysis, η_0 has been considered η .]

5. Non-Linear Schrodinger's equation and formation of rogue waves

For studying the generation of RW, we will setup Non-Linear Schrodinger Equation (NLSE). NLSE governs the dynamics of a wavepacket (envelope) such that dispersive effects are balanced by non-linear effects. Equation (43) can be extended to setup NLSE as shown below. Any field variable can be expanded in terms of Fourier series as follows:

$$F = \varepsilon^2 F + \sum_{s=1}^{\infty} \varepsilon_s (F_s e^{is\psi} + F_s^* e^{-is\psi}) \quad (44)$$

Where, F is the field variable, ε is the smallness parameter, and ψ is the phase factor. Now, using this equation we can expand the potential in equation (43) as,

$$\phi = \varepsilon^2 \phi_0 + \varepsilon \phi_1 e^{i\psi} + \varepsilon \phi_1^* e^{-i\psi} + \varepsilon^2 \phi_2 e^{2i\psi} + \varepsilon^2 \phi_2^* e^{-2i\psi} + \dots (45)$$

The first harmonics ϕ_1 and second harmonics ϕ_2 can be further expanded respectively:

$$\phi_1 = \phi_1^{(1)} + \varepsilon \phi_1^{(2)} + \varepsilon \phi_1^{(3)} + \dots (46)$$

$$\phi_2 = \phi_2^{(1)} + \varepsilon \phi_2^{(2)} + \varepsilon \phi_2^{(3)} + \dots (47)$$

Now, we use the change in variables as:

$$\rho = \varepsilon |\xi - c\tau| (48)$$

$$\theta = \varepsilon^2 \tau \quad (49)$$

Therefore, $\frac{\partial}{\partial \tau} = -is\omega - \varepsilon c \frac{\partial}{\partial \rho} + \varepsilon^2 \frac{\partial}{\partial \theta}$ and $\frac{\partial}{\partial \xi} = isk + \varepsilon \frac{\partial}{\partial \rho}$;

Where, s is the order of the wave equation ($s = 1$ for 1st order). By inserting the above terms in KdV Burger's equation after algebraic calculations we get the NLSE given by,

$$i \frac{\partial \phi}{\partial \theta} + P \frac{\partial^2 \phi}{\partial \rho^2} = -Q \phi \phi^* \phi (50)$$

Where, $P = -3kD$ and $Q = -\frac{N^2}{6Dk}$

The solution of equation (49) we get as,

$$\phi(\rho, \theta) = \sqrt{\frac{2P}{Q}} \left[\frac{4(1+4iPQ)}{1+16P^2Q^2+4\rho^2} - 1 \right] e^{-2iP\theta} (51)$$

By varying the variables ρ and θ we can get the rogue wave solution.

6. Dynamics of the system

Now we analyse the response of the ion acoustic system under normal conditions and under small periodic perturbations, its stability and its response to change in initial conditions, leading to its chaotic behavior.

6.1 Unperturbed system

Initially, the system is not under the influence of any external effects. Thus, the system is unperturbed.

From equation (35) we get the KdVB equation, as

$$\frac{\partial \phi}{\partial \tau} + N\phi \frac{\partial \phi}{\partial \xi} + D \frac{\partial^3 \phi}{\partial \xi^3} - R \frac{\partial^2 \phi}{\partial \xi^2} = 0$$

Using the transformation $\beta = \xi - M\tau$ (where M is the mach number, i.e. the phase velocity.) we get,

$$-M \frac{\partial \phi}{\partial \beta} + N\phi \frac{\partial \phi}{\partial \beta} + D \frac{\partial^3 \phi}{\partial \beta^3} - R \frac{\partial^2 \phi}{\partial \beta^2} = 0 \quad (52)$$

Integrating the equation, w.r.t., we get:

$$D \frac{\partial^2 \phi}{\partial \beta^2} = R \frac{\partial \phi}{\partial \beta} + M\phi - N \frac{\phi^2}{2} \quad (53)$$

Now,

$$\text{If } z = \frac{\partial \phi}{\partial \beta}, \quad (54)$$

Then equation (52) becomes,

$$D \frac{\partial z}{\partial \beta} = Rz + M\phi - N \frac{\phi^2}{2} \quad (55)$$

Solving equation (54) and (55) numerically, and studying its various plots, we can analyse the unperturbed system.

6.2 Perturbed system

We consider a small periodic perturbation force $f_0 \cos(\omega\eta)$. Thus equation (55) gets modified as,

$$D \frac{\partial z}{\partial \beta} = Rz + M\phi - N \frac{\phi^2}{2} + f_0 \cos(\omega\beta) \quad (56)$$

Solving equation (54) and (56) numerically, and studying its various plots, we can analyse the perturbed system.

7. Analytical Studies

A. From the dispersion relation, of the Electrostatic waves i.e. (14), (15), (16), (17) and, (18); we get the following 2-D plots:

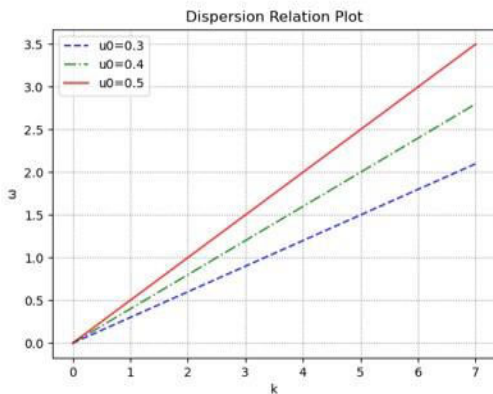


Fig. 1: Dispersion Relation plot of ESW for changing u_0 (u_0 =stream velocity), at constant η and μ .

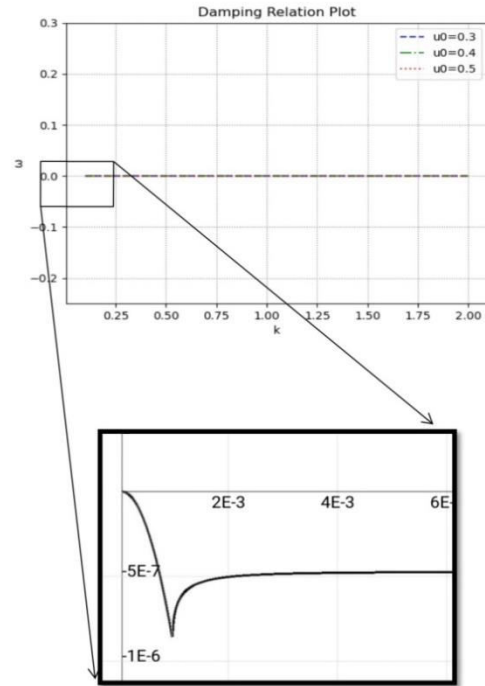


Fig. 2: Damping plot of ESW for changing u_0 (u_0 =stream velocity), at constant η and μ .

We see, from the dispersion relation curve of electrostatic waves, that almost from the beginning only, the DR plot attains constant linear growth, having constant slope u_0 (i.e. The stream velocity of the plasma particles).

From the damping plot also, we find, that initially there exists a changing non-zero damping effect, which exists for a very short time, after which the damping effects becomes constant, tending to zero.

B. From the dispersion relation of the Ion-acoustic waves (19), (20), (21), (22) and (23); we get the following 2-D plots:

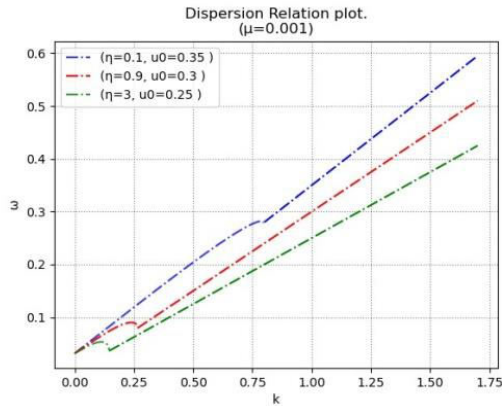


Fig. 3: Dispersion Relation plot of IAW for changing η (η = coefficient of viscosity), at constant μ .

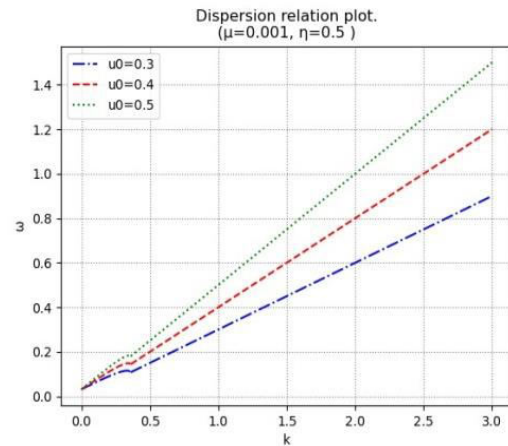


Fig. 5: Dispersion Relation plot of IAW for changing u_0 (u_0 = stream velocity), at constant η and μ .

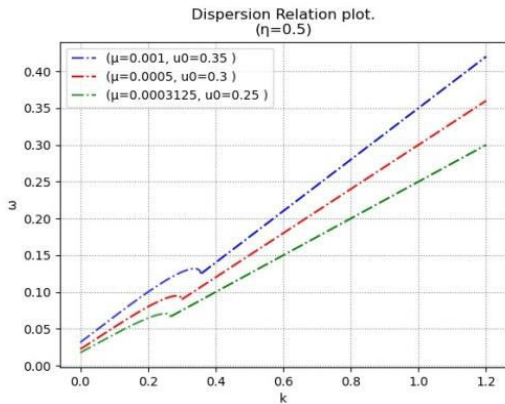


Fig. 4: Dispersion Relation plot of IAW for changing μ (μ = ratio between the mass of electron and the mass of ion), at constant η .

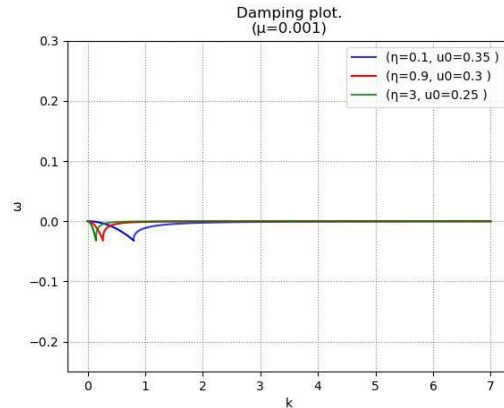


Fig. 6: Damping plot of IAW for changing u_0 (u_0 = stream velocity), at constant η and μ .

Analyzing the plots of the DR of Ion-acoustic waves, we find that the graph consists of two parts, one non-linear and one linear part. We observe, that the nonlinear part arises due to the square-root term present in the equation, and exists there, till k reaches the value $\sqrt[4]{\frac{4 \times \mu}{\eta^2}}$. After that, the graph attains constant linear growth.

If we graphically compute the gradient of the linear part, we see that the slope has the value of the stream velocity $[u_0]$ itself. Also, the slope is having constant value. Thus, we can say, that after a short time, the plasma attains a uniform velocity, equal to the stream velocity $[u_0]$. i.e. initially the group velocity decreases a bit, but then becomes as same as the value of stream velocity.

If we study the damping plot (Fig.6), (obtained from the imaginary part), we find, that initially there exists a non-zero damping effect, which reaches its maxima at $k = \sqrt[4]{\frac{4 \times \mu}{\eta^2}}$ and then, vanishes sharply, and becomes zero. This further confirms our analysis of the Dispersion relation plot (Fig. 5), and now we can correlate the two graphs together. As the damping effects increase, the group velocity is supposed to decrease, which is seen in the DR graph. Also, as soon as the damping effects start decreasing, the group velocity is supposed to attain constant value, as the plasma now moves with negligible hindrances. This also is confirmed by the DR graph, as we see, the group velocity attains a constant value u_0 .

From Fig. 4, we observe, that the initial (starting) group velocity increases with increasing value of μ ,

i.e., the initial velocity shows a slight increase with decreasing value of the mass of ions, (as $\mu=m_e/m_i$). This is quite justifiable, as ion mobility is inversely proportional to the ion mass.

From Fig.3, we see that, the nonlinear effects, decrease with increasing viscosity of the plasma, and thus, it is observed that the group velocity attains constant value faster in highly viscous plasmas, than in lowly viscous plasmas. Now, as density increases with viscosity, thus, we can say that as density increases, the nonlinear effects diminish faster. This can thus be attributed to the deby length of the plasma, which also decreases, on increasing density. So, the nonlinearity in the wave velocity is directly proportional to the deby length, and thus, we can say that the group velocity acquires a constant value faster, where the electric potential is neutralized faster.

C. From the solution of KdVB equation, (42) we get the following 2-D and 3-D plots for Electrostatic Waves and Ion-Acoustic Waves:

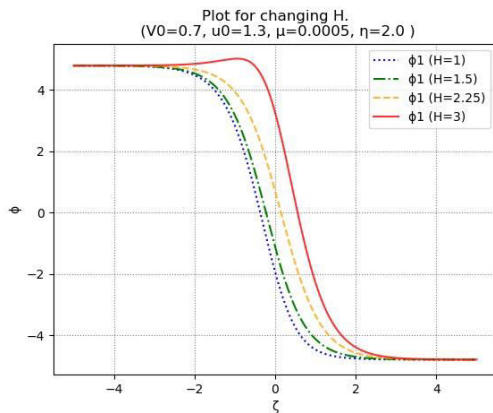


Fig. 7: Plot of the solution of the KdVB equation of ESW for changing H (H= Quantum Diffraction Parameter), at constant u_0, V_0, μ and η .

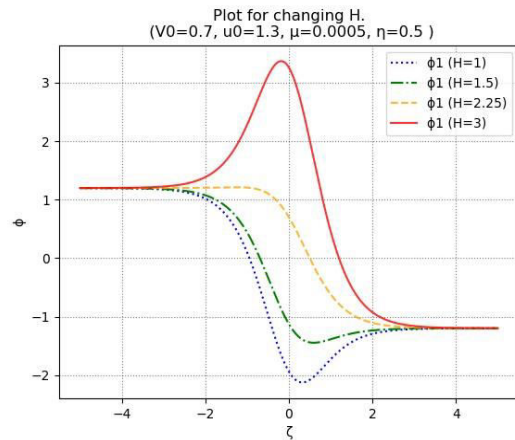


Fig. 8: Plot of the solution of the KdVB equation of ESW for changing H (H= Quantum Diffraction Parameter), at constant u_0, V_0, μ and η .

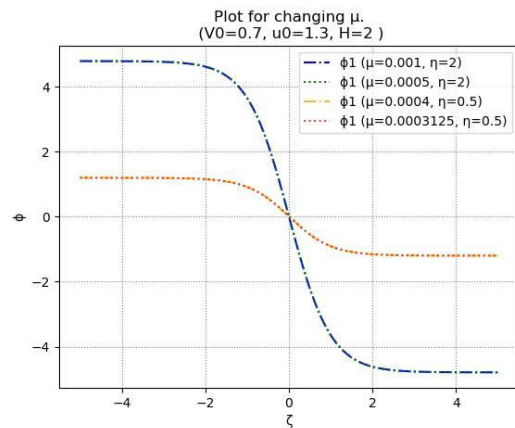


Fig. 9: Plot of the solution of the KdVB equation of ESW of different viscosity plasmas, for changing μ (μ = ratio between the mass of electron and the mass of ion), at constant u_0, V_0 and H.

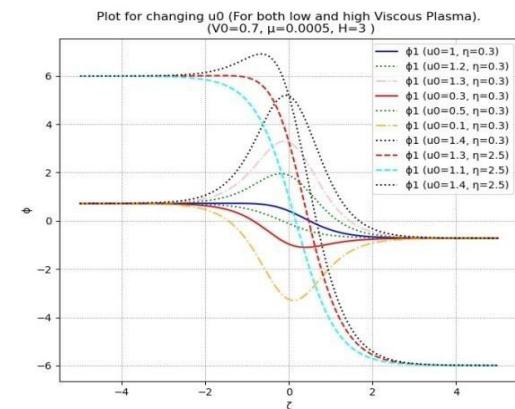


Fig. 10: Plot of the solution of the KdVB equation of

ESW of both highly and lowly viscous plasma, for changing u_0 (u_0 = stream velocity), at constant V_0, μ and H .

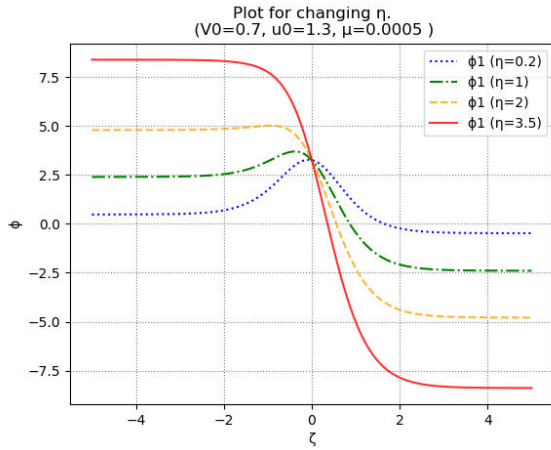


Fig. 11(a): Solitary profiles (2D) in plasma of ESW, for changing η (η = coefficient of viscosity), at constant u_0, V_0, μ and H .

KDVB surface plot
 (changing H ; $\eta=0.5, \mu=0.0005, u_0=1.3, V_0=0.7$)

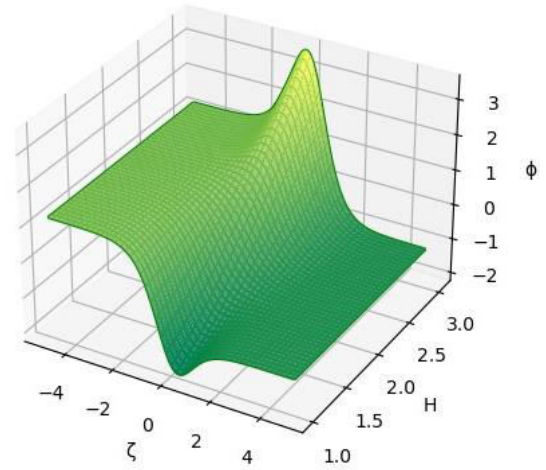


Fig. 12: Solitary profiles in plasma of ESW, for changing H (H = Quantum Diffraction Parameter), at constant u_0, V_0, η and μ .

KDVB surface plot
 (changing η ; $H=3, \mu=0.0005, u_0=1.3, V_0=0.7$)

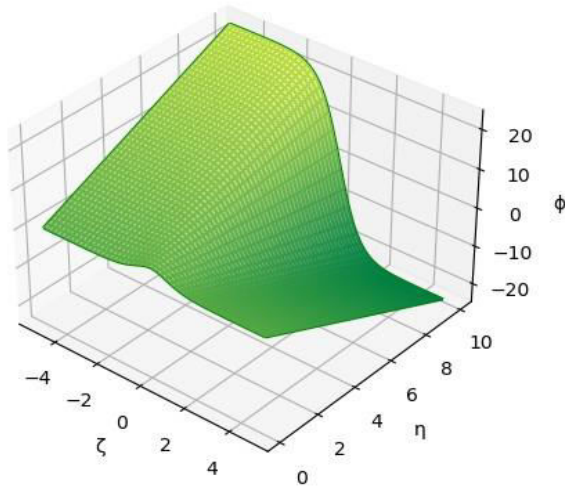


Fig. 11(b): Solitary profiles (3D) in plasma of ESW, for changing η (η = coefficient of viscosity), at constant u_0, V_0, μ and H .

KDVB surface plot
 (changing u_0 ; $H=3, \mu=0.0005, \eta=0.3, V_0=0.7$)

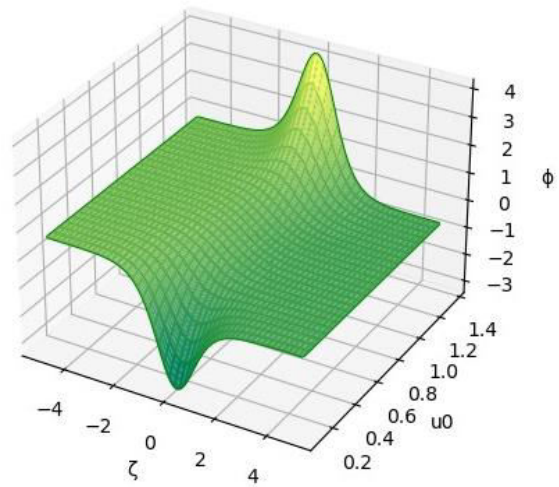


Fig. 13: Solitary profiles in plasma of ESW, for changing u_0 (u_0 = stream velocity), at constant V_0, μ, η and H .

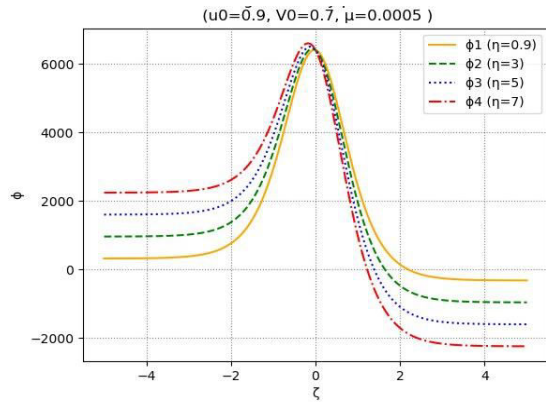


Fig. 14: Plot of the solution of the KdVB equation of IAW of highly viscous plasma, for changing η (η = coefficient of viscosity), at constant u_0, V_0 and μ .

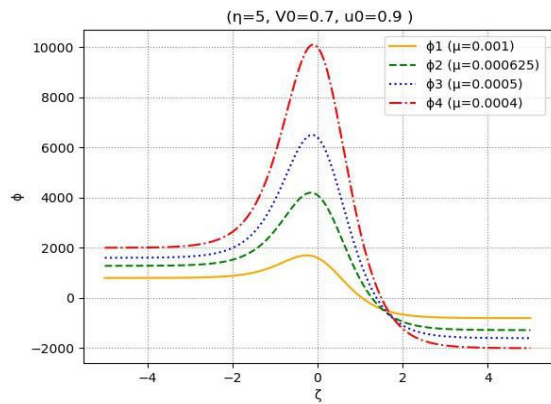


Fig. 15: Plot of the solution of the KdVB equation of IAW of highly viscous plasma, for changing μ (μ = ratio between the mass of electron and the mass of ion), at constant u_0, V_0 and η .

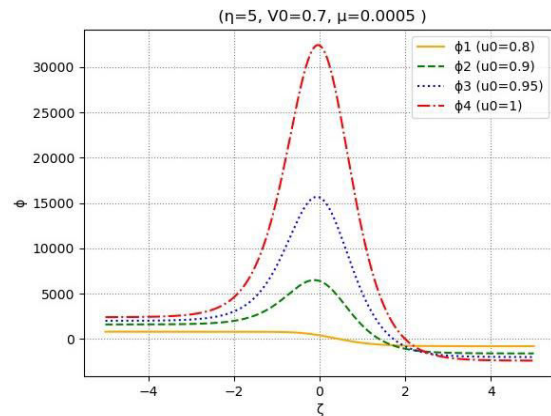


Fig. 16: Plot of the solution of the KdVB equation of IAW of highly viscous plasma, for changing u_0 (u_0 = stream velocity), at constant V_0, μ and η .

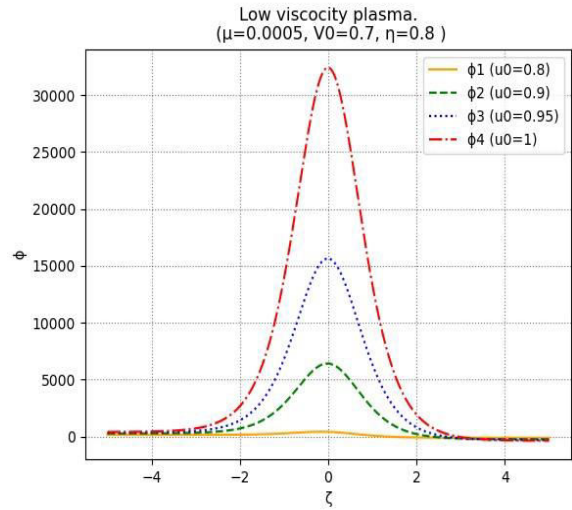


Fig. 17: Plot of the solution of the KdVB equation of IAW of lowly viscous plasma, for changing u_0 (u_0 = stream velocity), at constant V_0, μ and η .

KDVB surface plot
 (changing u_0 ; $\eta=5, V_0=0.7, \mu=0.0005$)

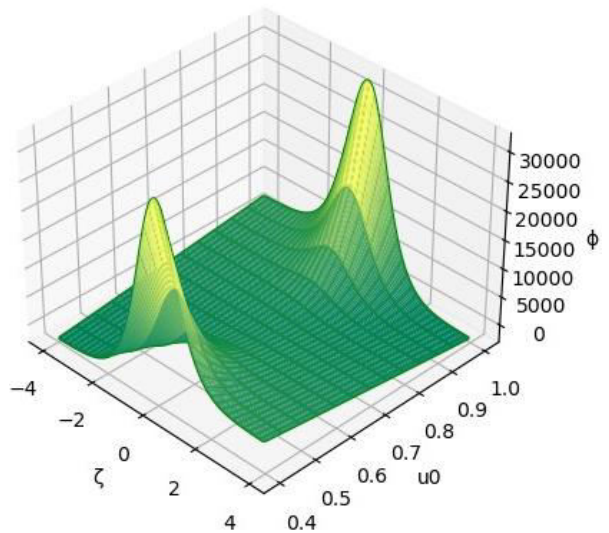


Fig. 18: Solitary profiles in plasma of IAW, for changing u_0 (u_0 = stream velocity), at constant V_0, μ and η .

(changing V_0 ; $\eta=5$, $u_0=0.9$, $\mu=0.0005$)

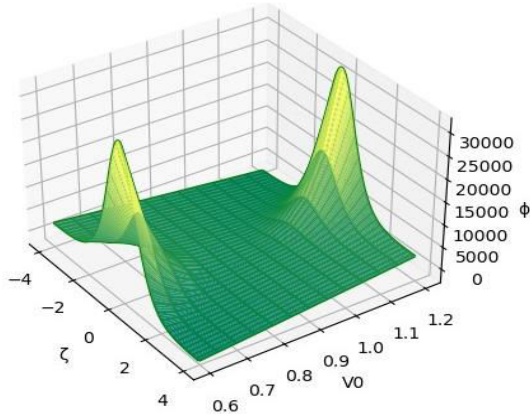


Fig. 19: Solitary profiles in plasma of IAW, for changing V_0 (= phase velocity) at constant u_0, μ and η .

(changing η ; $V_0=0.7$, $u_0=0.9$, $\mu=0.0005$)

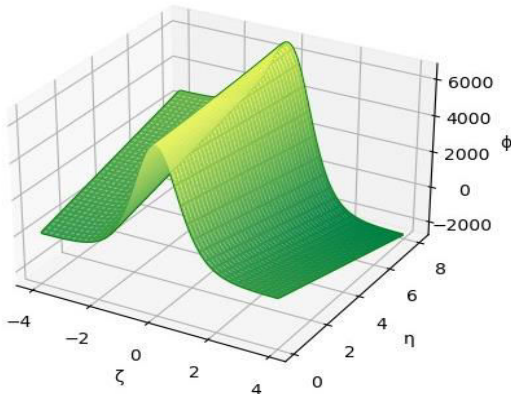


Fig. 20: Solitary profiles in plasma of IAW, for changing η (η = coefficient of viscosity), at constant u_0, V_0 and μ .

(changing μ ; $\eta=5$, $u_0=0.9$, $V_0=0.7$)

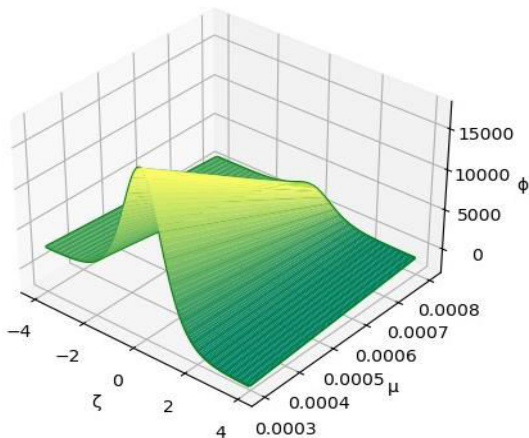


Fig. 21: Solitary profiles in plasma of IAW, for changing μ (μ = ratio between the mass of electron and the mass of ion), at constant u_0, V_0 and η .

From the 2D plots and 3D solitary profiles, of ESWs and IAWs, we observe that,

i) The height of the potential peak depends mainly on two factors, one, the difference between the phase velocity (V_0) and the stream velocity (u_0), and the second, on μ (i.e., the ratio between the mass of electron and the mass of ion).

ii) We observe that the symmetry of the curve gets distorted with the increase in coefficient of viscosity η_i . This can be attributed to the increase of the Shock properties in the solitary wave.

We see, that as viscosity increases, which increases the density; in comparison to the lowly viscous plasmas, in highly viscous plasma, initially there are a greater number of ions, which results in the initial rise of the positive potential with viscosity, on the left of the peak.

Also, the more the height of the potential peak, the more will be its interaction with the particles. As a result, higher peaked potentials repel the ions with more force and attract more negative charges, which results in the increase of negative potential on the right side of the peak.

Thus, more the abrupt change in the density, more will the solitary profiles tend to shock profiles.

iii) From fig. 15, fig. 19 and fig. 25, we observe, that for almost the same value of potential peak, the potential width drops rapidly with increasing viscosity. This observation is also justified, as, the higher the peak, the more number of electrons it will attract, thus resulting in the positive potential getting neutralised faster. Thus, resulting in the rapid decay of the potential peak.

iv) Also, there is a reversal in the sides of positive potential and negative potential, based on, whether the phase velocity (V_0) is greater than the stream velocity (u_0) or vice versa.

D. From the solution of NLSE of the Ion-Acoustic Wave (51), we get the following 2-D and 3-D plots of the function for Rogue Waves:

From the following plots we see that among a range of values for θ , (given in the legend of Fig. 22) only at one value of θ , the potential suddenly shoots up, and gets abnormally high (much higher than the peaks of the other solutions). This phenomenon depicts the formation of rogue waves, where a wave suddenly peaks up to the huge heights. Thus, having dangerous impacts on the surrounding systems.

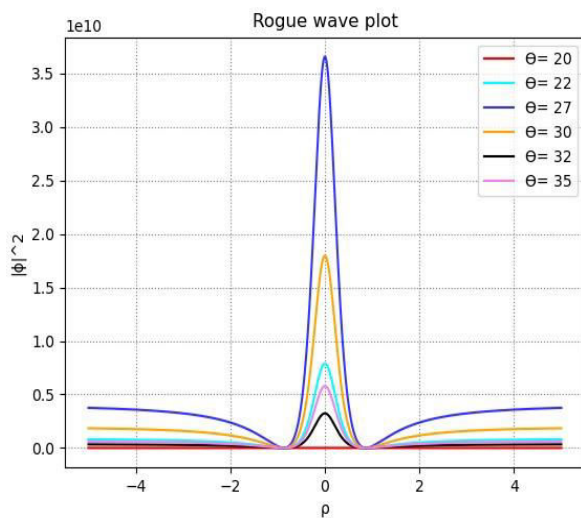


Fig. 22: 2D plot of the solution of the NLSE (Rogue Wave formation) for different values of θ

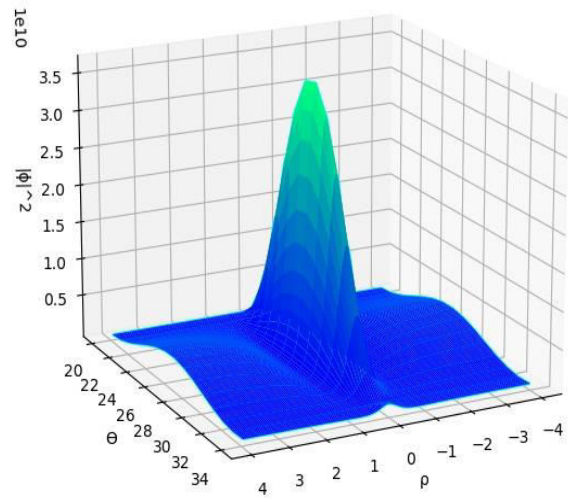


Fig. 23: 3D plot of the solution of the NLSE (Rogue Wave formation)

E. From the solution of equation (54), (55) and (56) we get the following 2-D and 3-D plots for studying the system under unperturbed and perturbed conditions:

a) For unperturbed states:

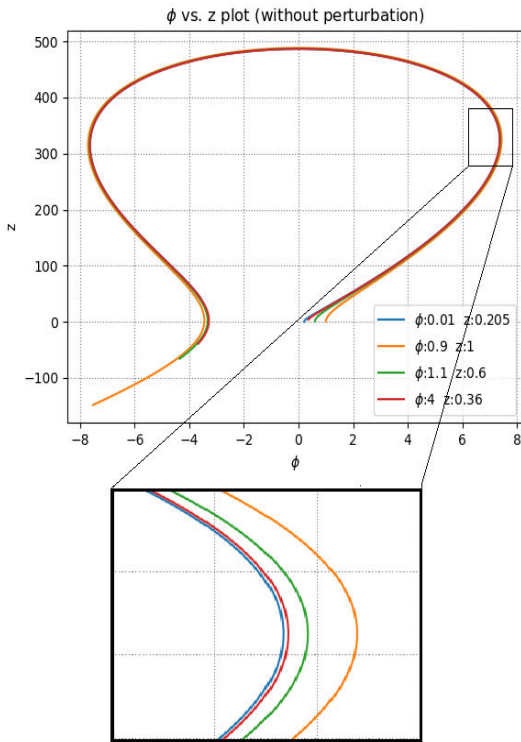


Fig. 24: Phase trajectory of the unperturbed system, (initial conditions in legend), plot of ϕ vs z , from equation (54) and (55) ($M=0.9$)

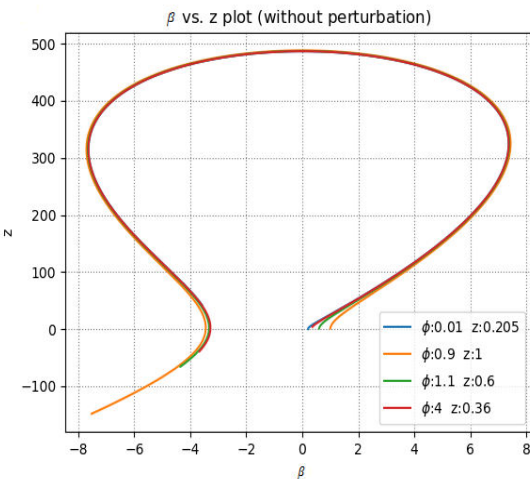


Fig. 25: Oscillation of the unperturbed system, (initial conditions in legend), plot of β vs ϕ , from equation (54) and (55) ($M=0.9$)

b) For perturbed states:

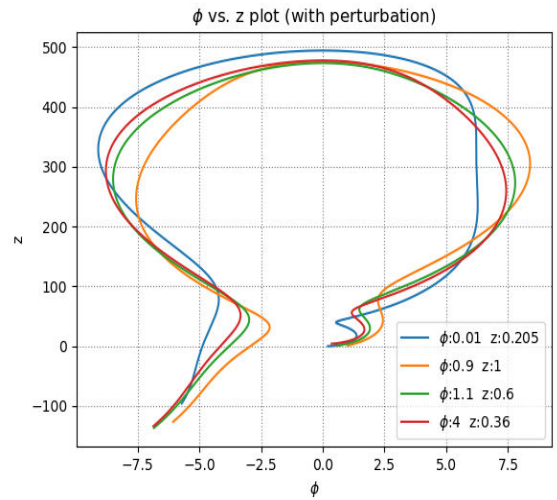


Fig. 26: Phase trajectory of the perturbed system, (initial conditions in legend), plot of ϕ vs z , from equation (54) and (56) ($M=0.9$)

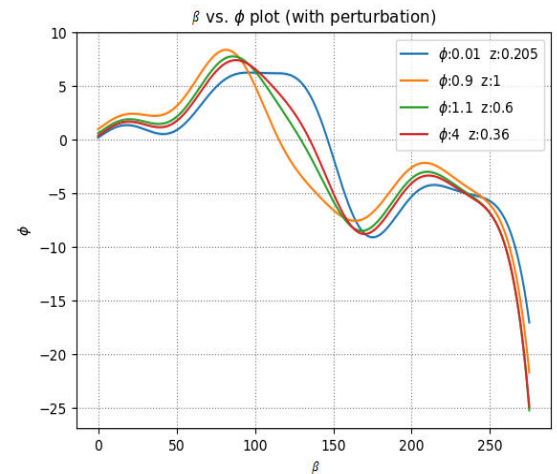


Fig. 27: Oscillation of the perturbed system, (initial conditions in legend), plot of β vs ϕ , from equation (54) and (56) ($M=0.9$)

From these plots of both the systems, we observe the following things:

- i) In case of the unperturbed system, the trajectory doesn't depend much on the initial conditions, except for the starting points. But in case of perturbed system, the change / distortion of trajectory with respect to the initial conditions can be visibly observed.

- ii) The periodic oscillation of the unperturbed system is highly systematic, but that of the perturbed system is chaotic and distorted.
- iii) Although distortion exists in the perturbed system, the basic outline (region) of the curve remains unaltered.
- iv) The phase trajectory initially appears to orbit around some central potential, but gets heavily and suddenly deflected outwards, near the end.

Thus, from these observations, we can infer that although the system appears to be stable initially, it loses its stability and tend to get chaotic in the long run. This might be due to the presence of hidden influencing forces, which remain passive initially, but gets active after a certain time, thus making the system unstable and chaotic. Thus, this work can be extended to the study of Lyapunov exponents, to assure the existence of hidden influencers.

7. Conclusions

From the detailed study of the plots, we analysed the basic properties of the Electrostatic and Ion-Acoustic waves in plasma, and noted their behavioral dependencies on different parameters like phase velocity, stream velocity, viscosity of the plasma and the ratio between mass of electrons and mass of ions. We observed that the greater the difference between the phase velocity, the higher the peak. Also, the more viscous a plasma, the faster the potential peak drops. And the lesser the mass of the ion, more is the effect of the potential peak on it. Thus, we can say, that due to the formation of such a positive potential peak in the plasma, the ions present are strongly repelled by it and are accelerated to supersonic velocities in a short span of time, giving rise to shock waves in plasma. Also, the more the height of the potential peak, the more will be its interaction with the particles. As a result, higher peaked potentials repel the ions with more force and attract more negative charges, which results in the increase of negative potential on the right side of the peak. From the solution of the nonlinear Schrodinger equation (NLSE) we can confirm the formation and presence of Rogue waves in the plasma. These sudden gigantic waves are destructive in nature, as their amplitudes are much larger than the ordinary waves, as can be seen from the graphical analysis. The occurrence of solar flares can also be attributed to similar phenomenon like this, where the particles attain supersonic velocities, traveling up all the distance

between sun and earth, and interfering with the Earth's atmosphere, where they interact with the particle present in the ionosphere. Due to collision the electrons present in those particles jump to excited states, and while returning to their initial states they radiate energy in the form of visible lights, resulting in the formation of auroras. The auroras are generally of green and blue color, which indicates the presence of nitrogen in the upper atmosphere of Earth. The occurrence of rogue waves in sun have got devastating effects on the artificial satellites moving in the outer space, as the occurrence of these waves are sudden, the satellites are unable to withstand or take safety measures against their damaging effects. The study of the system dynamics in both perturbed and unperturbed cases led to the inference that hidden forces may be present in the system, which leads to the system becoming chaotic and unstable in the long run.

Acknowledgments

The authors would like to thank the reviewers for their valuable inputs towards upgrading the paper. Further, authors would like to thank the Institute of Natural Sciences and Applied Technology, the Physics departments of Jadavpur University and Government General Degree College at Kushmandi for providing facilities to carry this work. We also acknowledge the cheers and suggestions of our parents and friends, especially D. Ghosh and A. De, whose timely suggestions and important inputs have helped us improve these works of ours.

References

- [1] B. Ghosh, S. Chandra, and S. Paul, "Amplitude modulation of electron plasma waves in a quantum plasma," *Physics of plasmas*, vol. 18, no. 1, p. 012106, 2011.
- [2] C. Das, S. Chandra, and B. Ghosh, "Nonlinear interaction of intense laser beam with dense plasma," *Plasma Physics and Controlled Fusion*, vol. 63, no. 1, p. 015011, 2020.
- [3] J. Sarkar, S. Chandra, and B. Ghosh, "Resonant interactions between the fundamental and higher harmonic of positron acoustic waves in quantum plasma," *Zeitschrift für Naturforschung A*, vol. 75, no. 10, pp. 819–824, 2020.
- [4] J. Sarkar, S. Chandra, J. Goswami, and B. Ghosh, "Formation of solitary structures and envelope solitons in electron acoustic wave in

- inner magnetosphere plasma with suprathermal ions,” *Contributions to Plasma Physics*, vol. 60, no. 7, p. e201900202, 2020. [Online]. Available: <https://onlinelibrary.wiley.com/doi/abs/10.1002/ctpp.201900202>
- [5] J. Goswami, S. Chandra, and B. Ghosh, “Shock waves and the formation of solitary structures in electron acoustic wave in inner magnetosphere plasma with relativistically degenerate particles,” *Astrophysics and Space Science*, vol. 364, no. 4, p. 65, 2019.
- [6] J. Sarkar, J. Goswami, S. Chandra, and B. Ghosh, “Study of small amplitude ion-acoustic solitary wave structures and amplitude modulation in epi plasma with streaming ions,” *LPB*, vol. 36, no. 1, pp. 136–143, 2018.
- [7] S. Chandra and B. Ghosh, “Non-linear propagation of electrostatic waves in relativistic fermi plasma with arbitrary temperature,” *Indian Journal of Pure & Applied Physics*, vol. 51, pp. 627–633, 2013.
- [8] B. Ghosh, S. Chandra, and S. N. Paul, “Relativistic effects on the modulational instability of electron plasma waves in quantum plasma,” *Pramana*, vol. 78, no. 5, pp. 779–790, 2012.
- [9] S. Chandra, S. N. Paul, and B. Ghosh, “Linear and non-linear propagation of electron plasma waves in quantum plasma,” *Indian Journal of Pure and Applied Physics*, vol. 50, no. 5, pp. 314–319, 2012.
- [10] B. Ghosh, S. Chandra, and S. Paul, “Amplitude modulation of electron plasma waves in a quantum plasma,” *Physics of plasmas*, vol. 18, no. 1, p. 012106, 2011.
- [11] P. Shukla and B. Eliasson, “Nonlinear instability and dynamics of polaritons in quantum systems,” *New Journal of Physics*, vol. 9, no. 4, p. 98, 2007.
- [12] S. Chandra and B. Ghosh, “Modulational instability of electron-acoustic waves in relativistically degenerate quantum plasma,” *Astrophysics and Space Science*, vol. 342, no. 2, pp. 417–424, 2012.
- [13] S. Chandra, S. N. Paul, and B. Ghosh, “Electron-acoustic solitary waves in a relativistically degenerate quantum plasma with two-temperature electrons,” *Astrophysics and Space Science*, vol. 343, no. 1, pp. 213–219, 2013.
- [14] U. Abdelsalam, W. Moslem, A. Khater, and P. Shukla, “Solitary and freak waves in a dusty plasma with negative ions,” *Physics of Plasmas*, vol. 18, no. 9, p. 092305, 2011.
- [15] A. Mamun and P. Shukla, “Electrostatic solitary and shock structures in dusty plasmas,” *Physica Scripta*, vol. 2002, no. T98, p. 107, 2002.
- [16] B. S. White and B. Fornberg, “On the chance of freak waves at sea,” *Journal of fluid mechanics*, vol. 355, pp. 113–138, 1998.
- [17] A. Saha, N. Pal and P. Chatterjee, *Phys. Plasma* 21,102101(2014)
- [18] B. Sahu, S. Poria and R. Roychoudhury, *astrophys. Space Sci.* 341,567(2012)

Received: 21st October 2020

Accepted: 21st December 2020

: